

ELECTRON-CLOUD MAPS FOR LHC SCRUBBING OPTIMIZATION

O. Domínguez*[†] and F. Zimmermann, CERN, Geneva, Switzerland

Abstract

Electron-cloud maps as alternative to detailed build-up simulations have already been applied in the past for a few accelerators, e.g. RHIC and the LHC at 7 TeV. We here report on a first application of maps to optimize the “beam scrubbing” of the LHC arcs at injection energy: Maps are used to efficiently determine the optimum bunch filling pattern which maximizes the electron flux on the chamber wall, while respecting constraints on the central cloud density to ensure beam stability. In addition, new features have been explored, e.g. by introducing thresholds which divide regions where either linear maps or cubic maps best describe the build-up and the decay of an electron cloud. In the near future we plan to extend the map formalism to individual slices in a dipole field in order to represent the vertical “stripes”.

INTRODUCTION

Electron multipacting processes in an RF cavity were first described by Farnsworth in the 1930's [1]. Inside the beam pipe of an accelerator, the time-varying electric field is provided by the beam and the primary electrons can be generated by a number of mechanisms (mainly beam residual gas ionization and photoemission). Depending on surface properties, beam pipe geometry and beam features, the primary electrons can gain enough energy to produce secondary electrons when hitting the chamber wall and provoke the build up of an electron cloud (EC). A good review of the detrimental EC effects in accelerators can be found in [2, 3].

Typically, EC simulations are being performed through thorough macroparticle tracking with specialized codes developed to this end (ECLLOUD, PyECLLOUD, CSEC, POSINST, etc.). A new approach was explored by Iriso and Peggs using a map formalism [4]. This allows describing the EC build up by means of a simple (cubic) algebraic maps which are capable of reproducing long filling schemes over millisecond time scales with an acceptable accuracy (e.g. peak and average values never differing by more than 15% from the results of a full-blown macroparticle simulation). Therefore, the map approach becomes a powerful tool to explore alternative bunch distributions fulfilling certain desired characteristics. This formalism has been successfully applied to RHIC [4], LHC dipoles at 7 TeV [5] and LHC dipoles and field free regions at injection energy [6].

The LHC mitigation strategy against EC includes several measures (a sawtooth pattern on the beam screen inside the cold arcs, NEG coatings, solenoids, etc.). However

these measures cannot be applied all along the machine and beam “scrubbing,” i.e. the bombardment of the beam-pipe surface with cloud electrons produced by the beam itself, is the ultimate solution to reduce the maximum Secondary Electron Yield (δ_{\max} , or just SEY), i.e. the number of secondary electrons per electron hitting the wall, to suppress multipacting and eventually to mitigate the detrimental electron cloud effects for the LHC (mainly excessive cryogenic heat load, large pressure rises and coherent plus incoherent instabilities). The effectiveness of the scrubbing process at the LHC has been demonstrated, especially for operation with a bunch spacing of 50 ns [7, 8]. However, when operating with beam parameters well above the SEY multipacting threshold, LHC EC activity hindered the storage or even the injection of some configurations with a bunch spacing of 25 ns (see e.g. [8]). Once this beam (typically made up of 72-bunch trains) was injected, beam losses and emittance growth rapidly diminished the scrubbing efficiency of such a beam configuration. Therefore it became interesting to explore alternative filling patterns which would maintain a better beam quality (thanks to lower electron peak flux and central density), while offering at the same time a similar electron dose as the default scrubbing beam.

In the following we report on how we have applied the map formalism to identify alternative filling schemes fulfilling the aforementioned conditions. As a new feature of the map approach, for this study we have introduced threshold values dividing regions where either linear maps or cubic maps, respectively, best describe the build-up and the decay of an electron cloud. In this paper we concentrate on the LHC cold arc dipoles since they occupy about 66% of the total machine circumference, and since most of the warm parts of the ring have been treated with low-SEY NEG coating, which suppresses any EC activity. All macroparticle tracking simulations have been carried out using PyECLLOUD.

LOW ELECTRON DENSITY REGIONS

After some scrubbing with a 25-ns bunch spacing beam in 2011, δ_{\max} in the LHC arcs was considerably reduced down to about 1.52 to be compared with a multipacting threshold of about 1.45 at injection energy [8]. After the annual winter shutdown 2012 some conditioning was expected to be lost. For this reason we mainly explored the situations for $\delta_{\max} = 1.6$ and $\delta_{\max} = 1.5$.

Studies cited in the previous section used the map formalism to explore filling schemes in order to minimize the EC effects in different accelerators. Nevertheless this is normally done in conditions well above the multipacting threshold. In this situation, thanks to the fast EC build up, very few (or no) points lie in the low electron density region

* Also at EPFL, LPAP, CH-1015 Lausanne, Switzerland

[†] octavio.dominguez@cern.ch

of the (ρ_{m+1}, ρ_m) space (see Fig. 1), where ρ_{m+1} designates the average electron density in the vacuum chamber after bunch m has passed by and ρ_m represents the electron density just before its passage. On the contrary, if we approach the SEY multipacting threshold (as it is the case for $\delta_{\max} = 1.5$ in the LHC arcs), we need a larger number of bunches to achieve saturation (i.e. to reach the identity map in Fig. 1) and more points lie in the low electron density region. Applying a cubic map to the entire region of the build up (map_{11}) we notice that the highest density points carry a relatively stronger weight in the fit. Zooming in on the low density region (see Fig. 1 bottom) reveals that the fit does not properly represent the simulated points here. Most importantly, it crosses the identity map ($\rho_{m+1} = \rho_m$ line), so that for low densities the map would imply a declining behaviour instead of the build up seen in the full simulation. A similar reasoning can be applied for the other periods of the electron-cloud evolution process, such as for the decay in the absence of beam (map_{00}) as well as for the “first empty bunch” map (map_{01}) (see e.g. [4] for map notation).

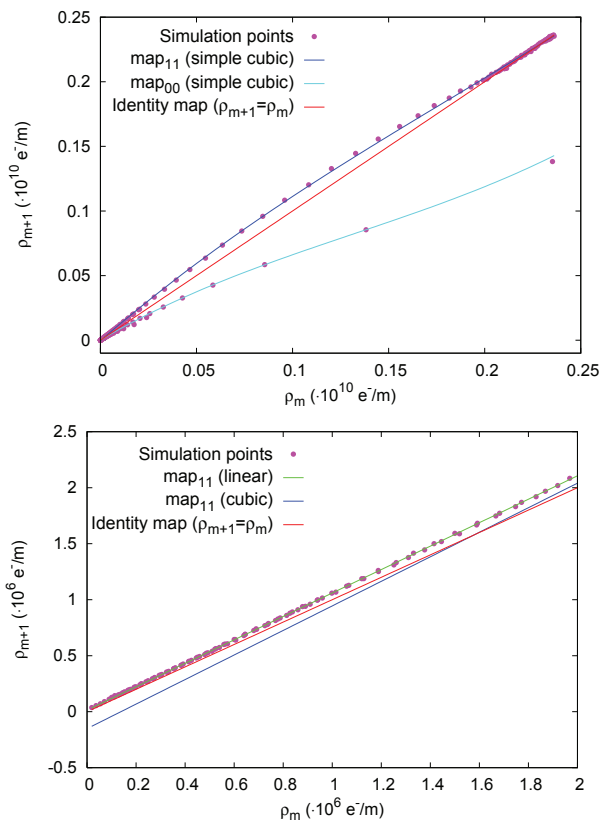


Figure 1: Cubic build-up and decay maps (map_{11} and map_{00} respectively) in the (ρ_{m+1}, ρ_m) space, showing the entire electron density region (top), and a zoom of build-up maps and simulation points in the low electron density region, showing that here the originally fitted cubic map (map_{11}) drops below the identity line, leading to an unphysical decay behaviour instead of a build up (bottom). In this region a linear map offers a better representation.

To avoid this unphysical behaviour we divided the points

for each map into two regions: A low density region, where a linear map properly fits the simulated points, and a high density region, where the usual cubic map is applied. The threshold separating both regions (for every map) is calculated as follows. We divide the simulated points corresponding to one map into two groups according to electron density. We then apply a linear map for the first group of points and a cubic map for the second and evaluate the quality of the fit by calculating the χ^2 . We repeat this for every possible split between low-density and high-density points. The partition with the smallest χ^2 value is considered optimum. It is worth mentioning that the “first full bunch” map (map_{10}) does not require this treatment since a simple linear map can always be applied here, for every case, thanks to its typically low density values.

SCRUBBING OPTIMIZATION

It has been shown that the map formalism can also be used for the modeling of the bunch-by-bunch electron flux impinging on the vacuum chamber walls [9]. All previous statements about maps for the electron density also apply to maps for the electron flux at the wall.

The higher the electron dose, the higher is the scrubbing efficiency and hence the faster the surface conditioning. On the other hand, a high EC activity also induces strong instabilities yielding beam losses and emittance blow up. This reduces dramatically beam life time and scrubbing efficiency.

The SPS (LHC main injector) can inject single batches of 72 bunches into the LHC. The minimum distance between batches is 925 ns (rise time of the LHC injection kicker). It is also possible to inject longer trains of up to four batches, spaced by 225 ns, with a minimum distance of 925 ns between groups of trains.

With imperfect surface conditioning, e.g. after a longer shutdown of a few months, it was difficult to directly inject the nominal LHC beam, consisting of 72 bunches per train. A high chromaticity (Q' in the order of 20 units) was necessary to ensure beam stability. The injection of 2-, 3- or 4-batch trains (which of course would yield higher electron dose rates) was not possible at all in this period. Such experience motivated us to consider filling patterns which would yield a better beam quality than the 72-bunch train (i.e. lower electron peak flux and central density) while at the same time offering a comparable electron dose.

Each LHC batch of 72 bunches is generated from initially 6 PSB bunches, which reach the SPS after having been split in 12 bunches each. This production scheme allows for a straightforward creation of a 12-bunch hole within an LHC bunch train by simply removing one injection from the PSB to the PS (see Fig. 2).

This flexibility can be exploited to develop filling schemes meeting our requirements. Figure 3 presents the integrated flux in one LHC turn at one location for different filling schemes showing a similar performance in terms of integrated electron dose with $\delta_{\max} = 1.6$ (likely to be closer to the initial situation after a longer shutdown).

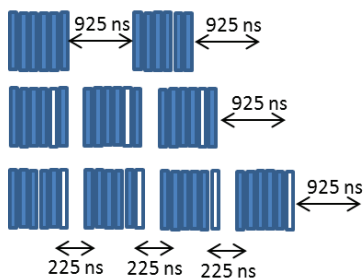


Figure 2: Sketch of some of the filling schemes studied. Empty boxes denote a missing injection from the PSB.

We can see that 4-batch trains skipping the fifth PSB injection, and 3-batch trains skipping the sixth one offer a scrubbing performance almost identical to the standard 72-bunch train, while 4-batch trains skipping the sixth injection increase the electron dose per turn by about 5%. The situation at $\delta_{max} = 1.5$, i.e. much closer to the multipacting threshold, is similar to the nominal 72-bunch train for the configurations in which we skip the sixth PSB injection (with a maximum difference of about 25% in integrated flux). Skipping any other injection would result in a much lower scrubbing efficiency and can therefore be discarded.

One indication of better beam stability can be given through the central electron density. The map formalism cannot be applied to this quantity directly. Figure 4 shows the central density for actual simulations of the standard filling scheme (72-bunch trains) and the alternative configuration offering the highest electron flux at $\delta_{max} = 1.5$, i.e. 4-batch trains skipping the last PSB injection in each batch. Average and peak central densities are 38% and 56% lower in the case of the alternative filling scheme. These values promise a better beam stability, while, considering the higher electron dose (about 22% from actual simulations), at the same time a higher scrubbing efficiency is expected. This injection scheme could be useful to maximize the electron dose during the first part of the scrubbing run. Once the surface conditioning reaches a level allowing the stable injection of standard 2, 3 or 4-batch trains with sufficient quality, these latter schemes are of course preferred.

Unfortunately, due to lack of time for the set up and a fast reconditioning which allowed injecting standard 4-batch trains rather quickly, we could not explore experimentally these filling schemes during the scrubbing run in December 2012.

SUMMARY

We have introduced a new approach to treat low electron density regions in the framework of the EC map formalism by establishing threshold values for the electron density, which divide the build up (or decay) phases into two density regions, the lower being described by a linear map and the higher by a cubic map. We have used this refined map approach to identify filling schemes which could optimize the scrubbing time of the LHC. Our target for this optimization has been to obtain bunch configurations offering an electron dose similar to the standard 25-ns single batch trains, while exhibiting lower peak and average cen-

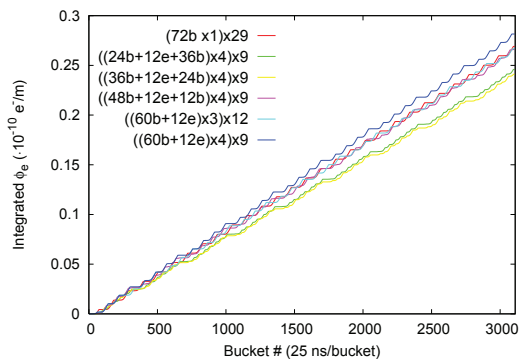


Figure 3: Integrated electron flux hitting the chamber wall for different filling schemes for an LHC turn at one location within an arc dipole using $\delta_{max} = 1.6$. In the legend, b denotes full bunches and e empty buckets. All the schemes generate a similar electron dose on the chamber wall. The flux was calculated using the refined the map approach.

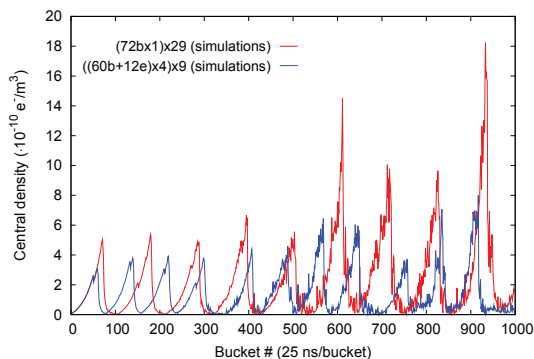


Figure 4: Central density for the standard filling scheme (red) and the proposed alternative scheme for scrubbing optimization (blue). Only a third of the machine is plotted to ease reading. The higher the central density the stronger the beam instabilities.

tral electron densities, thereby reducing the likelihood of beam instabilities, beam losses and resulting poor scrubbing efficiency. These schemes could not be experimentally tested during the 2012 scrubbing run due to several technical issues. Nevertheless these schemes can be reconsidered for the reconditioning after the present long 2013-14 LHC shutdown (“LS1”).

REFERENCES

- [1] P. Farnsworth, J. Franklin Inst., 218(4):411-444, Oct. 1934.
- [2] F. Zimmermann, Phys. Rev. ST Accel. Beams 7, 124801 (2004).
- [3] G. Rumolo *et al.*, Phys. Rev. ST Accel. Beams 4, 012801 (2001).
- [4] U. Iriso and S. Peggs, Phys. Rev. ST Accel. Beams 8, 024403 (2005).
- [5] T. Demma *et al.*, Phys. Rev. ST Accel. Beams 10, 114401 (2007).
- [6] O. Domínguez *et al.*, Proc. IPAC 2012, New Orleans, p. 3105.
- [7] O. Domínguez *et al.*, Phys. Rev. ST Accel. Beams 16, 011003 (2013).
- [8] G. Rumolo *et al.*, Proc. of the Chamonix 2012 Workshop, France, February 2012, pp.89.
- [9] T. Demma *et al.*, Proc. PAC’09, Vancouver, p. 4698.